Skeletal Radiol (2012) 41:1195–1212
DOI 10.1007/s00256-012-1427-0

REVIEW ARTICLE

The imaging of cartilaginous bone tumours. I. Benign lesions

H. Douis · A. Saifuddin

Received: 11 January 2012 / Revised: 18 March 2012 / Accepted: 23 April 2012 / Published online: 17 June 2012

Abstract Benign cartilage tumours of bone are the most common benign primary bone tumours and include osteochondroma, (en)chondroma, periosteal chondroma, chondroblastoma and chondromyxoid fibroma. These neoplasms often demonstrate typical imaging features, which in conjunction with lesion location and clinical history, often allow an accurate diagnosis. The aim of this article is to review the clinical and imaging features of benign cartilage neoplasms of bone, as well as the complications of these lesions.

Keywords Benign chondral lesions · Osteochondroma · Enchondroma · Chondroblastoma · Chondromyxoid fibroma · Imaging

Introduction

Benign cartilage tumours are the most common primary bone tumours constituting approximately 24% of all such lesions and include osteochondroma, (en)chondroma, chondroblastoma and chondromyxoid fibroma. Whilst osteochondroma and enchondroma are very common benign cartilage lesions, which are usually asymptomatic and often discovered incidentally, chondroblastoma and chondromyxoid fibroma are rare benign cartilage tumours that usually present with pain. The majority of these lesions can confidently be diagnosed based on a combination of clinical findings, lesion location and imaging characteristics. It is therefore vital for radiologists, clinicians and pathologists alike to be familiar with the clinical characteristics and imaging features of these tumours in order to establish the correct diagnosis, thereby avoiding unnecessary biopsy, which in some instances could potentially be misleading and even harmful.

The aim of this review article is to provide an overview of the epidemiology, clinical presentation, typical location, potential complications and imaging findings of benign cartilage tumours.

H. Douis (✉) · A. Saifuddin
Department of Radiology, The Royal National Orthopaedic Hospital NHS Trust,
Brockley Hill,
Stanmore, Middlesex HA7 4LP, UK
e-mail: douis.hassan@gmx.de

Osteochondroma

Osteochondroma (OC), also termed exostosis, represents the commonest benign bone tumour, accounting for 10–15% of all osseous neoplasms and 20–50% of benign bone tumours [1, 2]. It is also the commonest bone tumour in children. The lesion may be solitary or multiple, the latter condition being termed diaphyseal aclasis or hereditary multiple exostoses (HME). In a single-centre study of 382 cases, 313 (82%) were solitary while 69 (18%) were associated with HME [3].

It has long been postulated that sporadic osteochondromas are developmental in origin. However, recent studies have revealed that mutations in the gene encoding exostosin 1 (EXT1) are associated with solitary osteochondromas, which would support the theory that they are true neoplasms [4]. EXT1 and EXT2 are proteins involved in the synthesis of heparan sulphate proteoglycans (HSPG). In the growth plate, HSPGs bind to Indian hedgehog ligands in the extracellular environment, thereby controlling the diffusion of hedgehog ligands. Mutations in the EXT genes lead to abnormal HSPG processing and the accumulation of HSPG

in the cytoplasm of chondrocytes. The lack of extracellular HSPG results in an abnormal diffusion of Indian hedgehog ligands in the extracellular environment, resulting in a larger area in which Indian hedgehog can diffuse. This change in diffusion area has been postulated to lead to a loss of polar organization, allowing growth-plate chondrocytes to grow in the wrong direction [5, 6].

Continued growth of these chondrocytes with subsequent endochondral ossification results in the formation of an outgrowth of both medullary and cortical bone covered by a cartilaginous cap of variable thickness. It is the continuity of the medullary cavity with that of the underlying bone of origin that is pathognomonic of the lesion [1, 2]. Typically, the lesion continues to grow until skeletal maturity.

Osteochondromas can develop following surgery and Salter–Harris fractures [2]. OC represents the commonest benign radiation-induced bone tumour, with various series reporting such development in 6–24% of irradiated patients [2]. OC development has been described in 24% of children under the age of 5 years who received total body irradiation prior to bone marrow transplantation, the lesion arising at a mean of 4.6 years after treatment [7]. Similarly, the development of osteochondromas has been associated with haematopoietic stem cell transplantation. [8]. A large retrospective study that evaluated the incidence and risk factors for the development of osteochondromas in 1,632 children treated with haematopoietic stem cell transplantation ± total body irradiation for malignancies found that osteochondromas occurred in 27 patients who underwent haematopoietic stem cell transplantation. According to this study, the 5-, 10- and 15-year cumulative risk of developing OC after treatment was 0.5%, 3.2%, and 6.1% respectively. However, multivariate analysis revealed that younger age at the time of haematopoietic stem cell transplantation and total body irradiation were the only factors that were significantly associated with the development of OC, whilst autologous stem cell transplantation was found to be a less significant risk factor. The authors therefore postulated that autologous stem cell transplantation was a confounding factor and that the above findings were not due to autologous stem cell transplantation "per se", but due to the fact that 95% of the patients who developed OC after autologous stem cell transplantation also underwent total body irradiation [9].

Solitary OC is estimated to occur in 1–2% of the population and the vast majority are asymptomatic [2]. Symptomatic lesions tend to occur in younger individuals, with approximately 75% of such cases arising before the age of 20 years [2]. They are more common in males by a ratio of 1.4 to 3.6 [2]. Approximately 50% of OC arise in the lower limb, with 40% occurring around the knee joint. The femur is the commonest bone involved (30% of all cases) with 75% of femoral lesions arising distally. The humerus is involved in 10–20% of all cases. Rarer locations include the small bones of the hands and feet (10%), the scapula (4%) and the pelvis (5%) [2]. Within the carpus, lesions of the scaphoid [10] and lunate [11] have been described. In the hindfoot, the calcaneus [12] and talus [13] may be involved, while sub-ungual lesions may occur in the forefoot [14].

The commonest presentation is with a non-tender, slowly growing bony lump. Complications associated with OC include deformity, fracture, overlying bursa formation and compression of adjacent soft tissue structures, particularly nerves and vessels. Malignant transformation is the most serious complication and occurs in approximately 1% of solitary osteochondromas [2]. Pain associated with OC may also be due to infarction of the cartilage cap or secondary infection [1].

Bone deformity is not only caused by the lesion itself, but may also be due to growth disturbance (metaphyseal undertubulation) and bowing. Also, deformity of an adjacent bone can occur, particularly in the paired bones of the forearm and lower limb, as well as the ribs from an OC arising on the deep surface of the scapula. Synostosis between paired bones has also been described [15].

Fracture is an unusual complication of trauma to an OC and most commonly occurs around the knee at the base of a pedunculated lesion [16]. Surgical resection of the fractured fragment may be required, although spontaneous resorption has been described [2].

Bursa formation overlying the cartilage cap of an exostosis occurs with a reported incidence of 1.5% [2] and may mimic malignant transformation. It occurs most commonly in association with scapular lesions [17] and those arising from the lesser trochanter of the femur. Bursal osteochondromatosis is a recognised complication of bursa formation [18].

Vascular complications associated with OC include vessel displacement, stenosis, occlusion and pseudoaneurysm formation [2]. Simple vessel displacement is usually asymptomatic, while stenosis/occlusion can result in distal limb ischaemia and also popliteal artery entrapment syndrome [19]. Pseudoaneurysm presents as a pulsatile mass and may involve the popliteal [20] and superficial femoral arteries [21]. Compression of a variety of neural structures, including the sciatic nerve [22], common peroneal nerve [23, 24] and radial nerve [2] has also been described. Lesions arising around the shoulder joint can be complicated by rotator cuff impingement [25], subscapularis tear [26] and bicipital tendonitis [27].

Malignant transformation of OC occurs within the cartilage cap, resulting in the development of a secondary (peripheral) chondrosarcoma. Rarely, however, OC may be complicated by the development of other malignant tumours, such as osteosarcoma [28].

Osteochondroma can be managed conservatively, if small and asymptomatic, or by surgical resection through its base [1, 2]. Failure to resect the complete perichondrium can result in local recurrence, which has been reported in 2–5% of cases [2, 29]. Rarely, spontaneous resolution may occur [30].

The radiological features of OC are commonly pathognomonic [1, 2], comprising a well-defined bony mass composed of both a medulla and overlying cortex, which is continuous with the underlying bone. The base of the lesion may be broader than the lesion itself, in which case the OC is termed "sessile" (Fig. 1) or it may be slim with an expanded head, when the lesion is termed "pedunculated" (Fig. 2). Such lesions typically arise in a metaphyseal/metadiaphyseal location and point away from the adjacent joint. Lesion continuity with the bone of origin is usually clearly seen radiographically for long bone OC (Figs. 1a, 2a), but for those arising from flat bones, commonly requires cross-sectional imaging such as CT or MRI (Fig. 3). Pathologically, the whole lesion varies from 1 to 10 cm in size [2]. In contrast, the cartilage cap thickness is less than 2 cm when measured perpendicular to the osteochondroma. A cap thickness of more than 2 cm in adults is associated with an increased likelihood of malignant transformation to chondrosarcoma. These features are optimally assessed by cross-sectional imaging.

Although the cartilage cap is easily measured when small and uniform (Figs. 1b, 2c), it is difficult to obtain accurate and reliable measurements if the cap is convoluted or irregular. Recently, Bernard and co-workers retrospectively evaluated the cartilage cap thickness on CT and MRI in 67 histologically proven osteochondromas and 34 histologically proven exostotic (secondary) chondrosarcomas and correlated the cap thickness on CT and MRI with the gross pathological findings in 32 cases (26 osteochondromas; 6 chondrosarcomas). They proposed the following technique for the measurement of cartilage cap thickness: the cap thickness is measured by identification of the tidemark of low-signal-intensity mineralization that serves as a boundary between the medullary cavity and the overlying cartilage. A connecting line is then drawn between adjacent peaks in the tidemark undulations. Crevasses of cartilage between tidemark undulations are subsequently excluded. The thickest portion of the cartilage is then measured perpendicular to the tidemark. Using this technique, they found measurement variances of 3 mm or less when correlating cap thickness on imaging with that on gross pathological specimens. Furthermore, Bernard et al. found that a cut-off value for the cartilage cap thickness of 2 cm in the differentiation of osteochondromas from chondrosarcomas led to 100% sensitivity, 98% specificity on MRI and 100% sensitivity, 95% specificity on CT [31].

The scintigraphic appearance of OC is dependent upon the activity of endochondral bone formation and as such, OC in the skeletally immature may show increased activity, while those imaged after skeletal maturity may show minimal abnormality [2].

Computed tomography is the optimal technique for demonstrating lesion continuity, particularly in areas of complex anatomy such as the shoulder girdle, pelvis (Fig. 3b) and hip (Fig. 4a) and also clearly identifies the typical chondral calcifications of the cartilage cap. The thickness of the cartilage cap can be difficult to assess with CT, since it may be isodense to overlying skeletal muscle or a complicating bursa. However, relatively large cartilage caps,

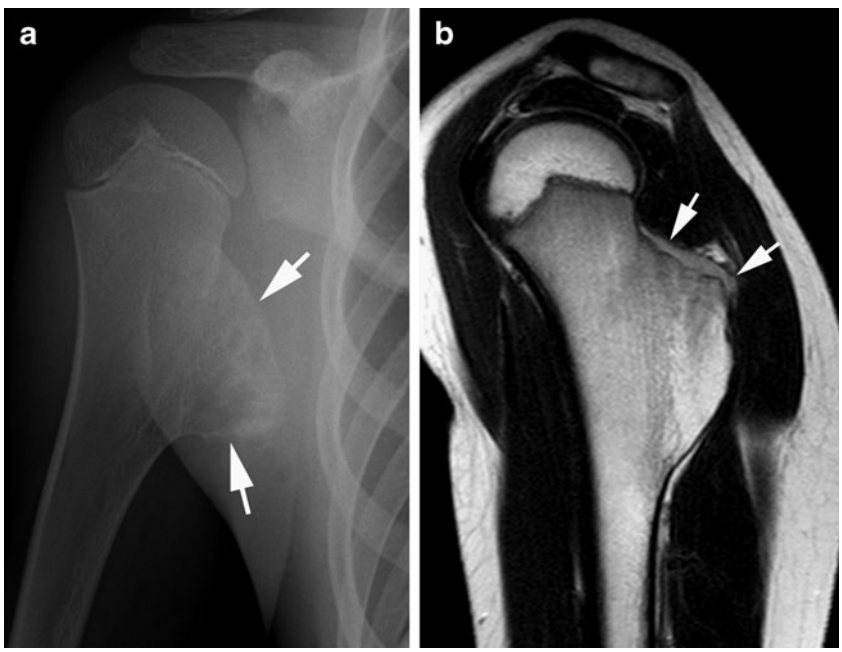

Fig. 1 Sessile osteochondroma of the humerus. **a** Anteroposterior radiograph of the shoulder demonstrates a broad-based sessile osteochondroma (*arrows*) that arises from the medial humeral metaphysis. **b** Sagittal T2W FSE MR image shows medullary continuity between the lesion and the native humerus. The cartilage cap is hyperintense (*arrows*)

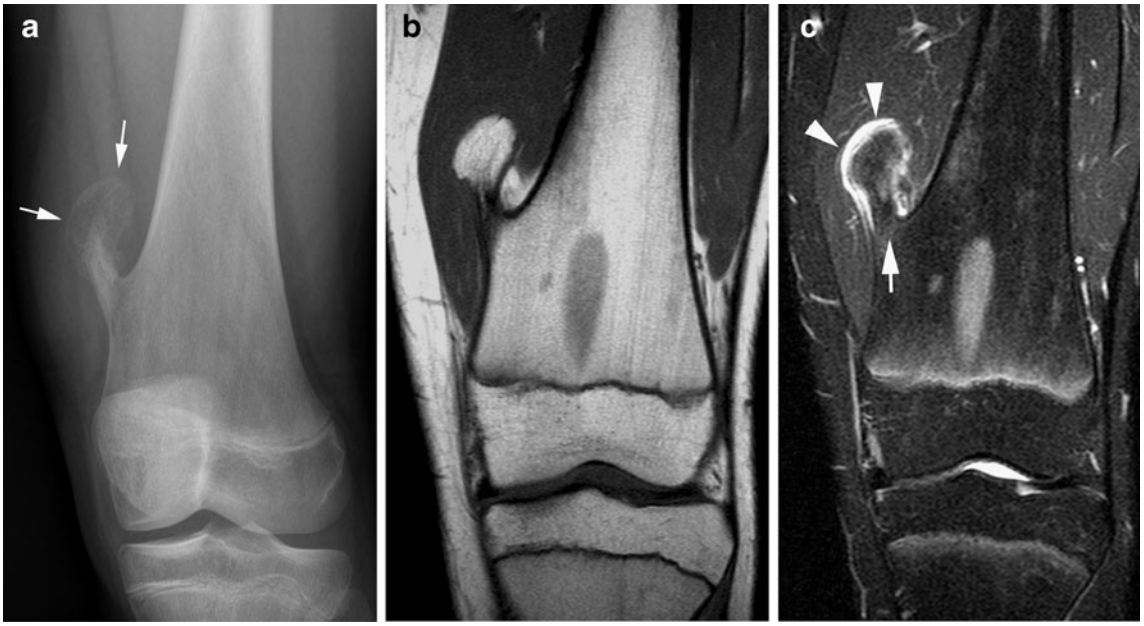

Fig. 2 Pedunculated osteochondroma of the femur. **a** Anteroposterior radiograph of the knee demonstrates a pedunculated osteochondroma (*arrows*) that arises from the medial femoral metaphysis. **b** Coronal T1W SE MR image shows the cap of the lesion to be isointense to adjacent skeletal muscle. **c** Coronal STIR MR image shows medullary continuity between the osteochondroma and femur through its stalk (*arrow*). Note that the cartilage cap is thin and uniformly hyperintense (*arrowheads*)

because of their high water content, are slightly hypodense to muscle and can be accurately assessed [2].

Ultrasound has also been shown to be of value in assessing cap thickness, the cartilage cap appearing hypoechoic with areas of punctuate or linear hyperechogenicity representing matrix calcification [2].

Magnetic resonance imaging is of undoubted value in assessing all aspects of OC, including medullary continuity (Figs. 1b, 2c, 4b), cartilage cap thickness (Figs. 1b, 2c) and the previously mentioned complications [1, 2, 32, 33]. The base of the OC has the typical appearance of normal bone, with a hypointense thin outer cortex and central medullary fat SI. We have also noticed areas of red marrow-like SI within the bony stalk (Fig. 5a, b), a relatively common feature that may be related to patient age. The junction of the bony stalk with the cap is typically undulating, with areas of chondral tissue commonly extending into the medullary cavity of the lesion. The cap has typical MRI features of well-differentiated hyaline cartilage, appearing to be of low-intermediate SI on T1W images (Fig. 2b) and markedly hyperintense on T2W images (Figs. 1b, 2c), which are therefore the best for distinguishing the cap from adjacent muscle. Hypointense internal septa are commonly identified. It should be noted that the cap may appear very heterogeneous in the younger individual, while it is still undergoing active endochondral ossification [2]. The cap

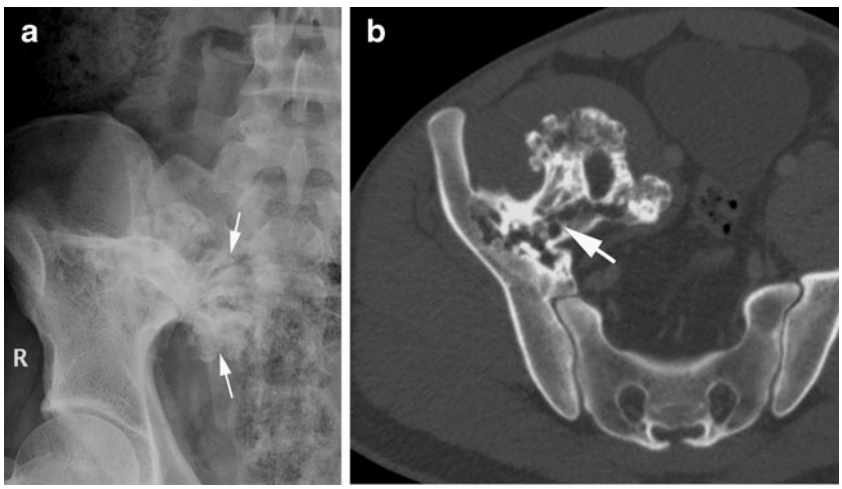

Fig. 3 Osteochondroma of the right ilium. **a** Anteroposterior radiograph of the right hemipelvis and hip shows a heavily mineralised irregular lesion (*arrows*) overlying the right iliac blade. **b** Axial CT study shows the lesion to be arising from the inner aspect of the right ilium with continuity between the medullary cavities (*arrow*)

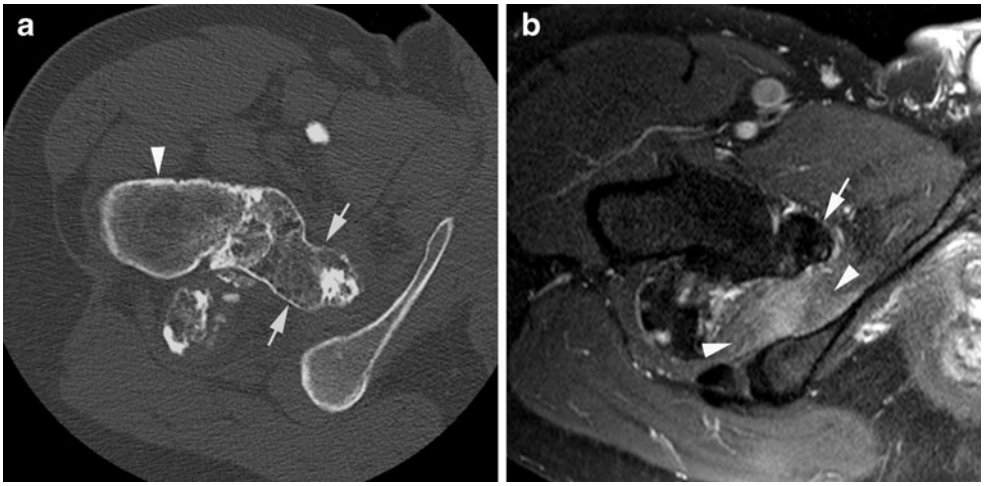

Fig. 4 Osteochondroma of the right proximal femur. **a** Axial CT study demonstrates medullary continuity between the osteochondroma (*arrows*) and the native femoral neck (*arrowheads*). **c** Axial fat-suppressed PDW FSE MR image shows oedema of the quadratus femoris muscle (*arrowheads*) due to impingement between the osteochondroma (*arrow*) and the ischium

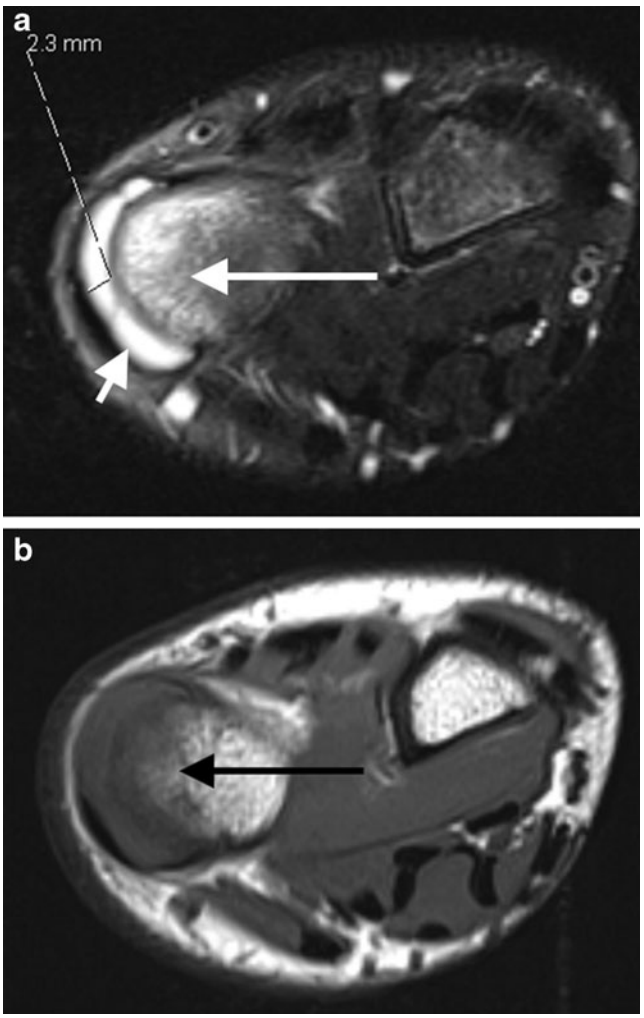

Fig. 5 Osteochondroma of the left distal ulna. **a** Axial fat-suppressed T2W FSE MR image shows the hyperintense cartilage cap (*small arrow*) and red marrow-like SI within the stalk (*long arrow*). **d** The corresponding axial T1W FSE MR image confirms red marrow-like SI within the stalk (*long arrow*)

is commonly bordered by a thin hypointense line, which represents the perichondrium. Typical septal and peripheral enhancement is seen following gadolinium [2].

Magnetic resonance imaging is the technique of choice for imaging the complications of OC [32, 33]. The mechanical effects of the lesion on overlying muscle may result in oedema (Fig. 4b), which can also be due to denervation and is manifested as increased T2W SI with or without associated atrophy [33] (Fig. 6). In the appendicular skeleton, the majority of neurological complications occur around the knee, particularly involving the common peroneal nerve. MRI will demonstrate denervation and/or atrophy of the short head of the biceps femoris, and the anterior and lateral

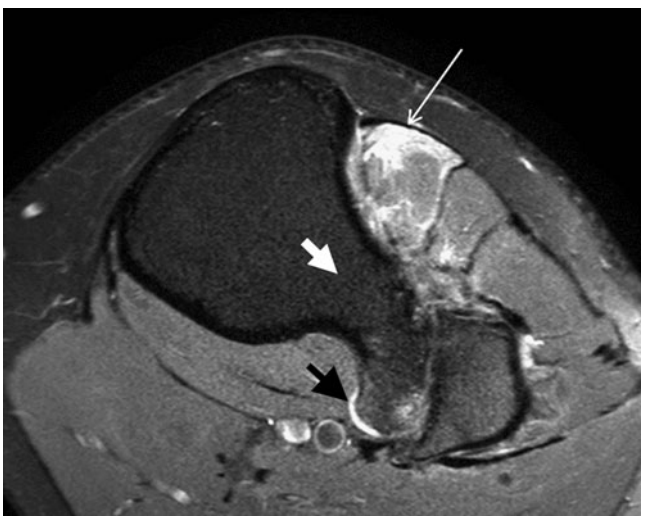

Fig. 6 Osteochondroma of the proximal right tibia. Axial fat-suppressed T2W FSE MR image shows bony synostosis (*small thick white arrow*) between the proximal tibia and fibula due to an osteochondroma and denervation oedema of the tibialis anterior muscle (*long thin white arrow*). Note the thin cartilage cap of the osteochondroma (*small thick black arrow*)

compartment muscles of the calf [33]. Bursa formation can also be demonstrated, appearing as an irregular fluid-filled lesion (Fig. 7) that may contain debris or chondral loose bodies and shows rim enhancement following gadolinium. The fluid nature of the lesion can also be demonstrated by ultrasound [33]. The mechanical effects on adjacent bones (bowing, erosion, pseudarthrosis, synostosis) are usually demonstrated radiographically, but can be optimally characterised with CT (Fig. 8) [33].

Pseudoaneurysm formation most commonly occurs in the setting of a sessile OC causing chronic friction against the vessel, most commonly the popliteal artery. The pseudoaneurysm has typical appearances on MRI, including relationship to the vessel of origin, pulsation artefact (Fig. 9a) and an "onion-like" laminated appearance due to the deposition of haemosiderin between layers of vascular thrombus. MR angiography is as good as conventional angiography or CT angiography (Figs. 9b) in the assessment of pseudoaneurysms arising from medium and large vessels [33].

Fig. 8 Osteochondroma of the distal left tibia. Coronal CT MPR showing a sessile osteochondroma of the lateral metaphysis causing pressure erosion and bowing of the adjacent fibula

(En)chondroma

Chondroma or enchondroma represents a benign neoplasm of hyaline cartilage and is the second commonest benign chondral tumour following osteochondroma [34–37]. It is widely postulated that enchondromas arise because of the displacement of embryonic rests of cartilage from the growth plate into the metaphysis. Involvement of multiple growth plates is thought to result in enchondromatosis (Ollier disease; Maffucci syndrome) [34]. However, the pathogenesis of solitary enchondromas of long bone has recently been challenged by Douis and co-workers, who retrospectively evaluated 240 MRI examinations of the knee performed in 209 children. They failed to identify displacement of cartilage into the metaphysis on MRI in their cohort, therefore questioning this widely believed theory [38]. Furthermore, a study by Amary and co-workers identified somatic mutations in isocitrate dehydrogenase 1 and 2 in 52%

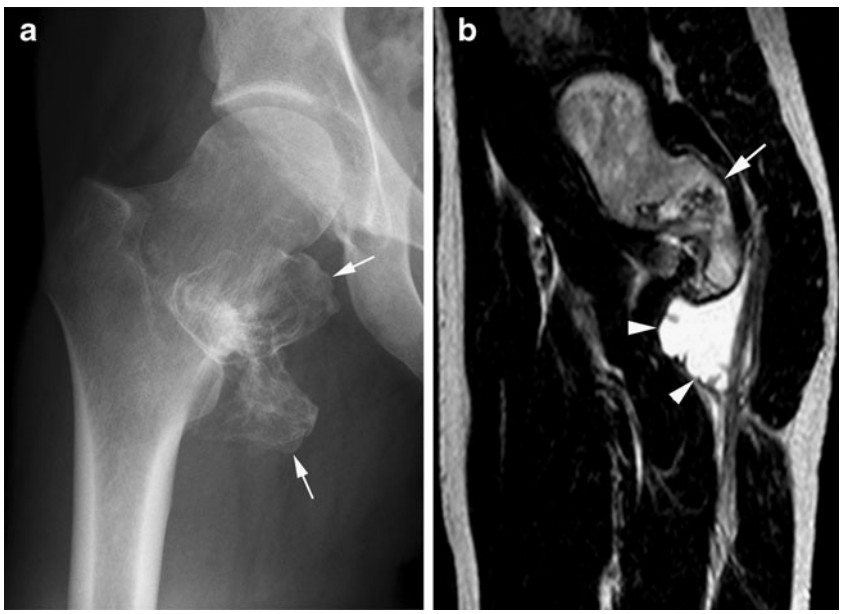

Fig. 7 Osteochondroma of the proximal right femur. **a** Anteroposterior radiograph of the right hip demonstrates an osteochondroma (*arrows*) that arises from the posteromedial aspect of the femoral neck. **b** Sagittal T2W FSE MR image shows the sessile lesion (*arrow*) and bursa formation (*arrowheads*) adjacent to its inferior pole

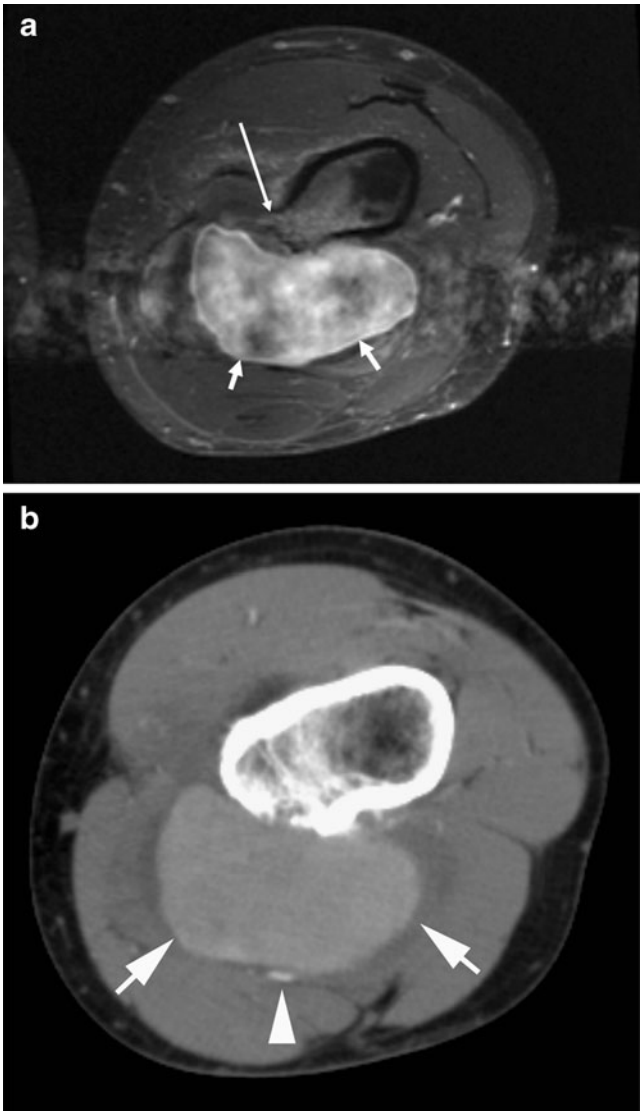

Fig. 9 Osteochondroma of the right femur. **a** Axial fat-suppressed T2W FSE MR image shows a sessile osteochondroma (*long arrow*) that arises from the posteromedial aspect of the distal femur. An irregular oval hyperintense mass (*small arrows*) is noted posterior to the lesion, through which there is prominent transverse pulsation artefact. **b** Axial post-contrast CT study shows the compressed popliteal artery (*arrowhead*) and the enhancing pseudoaneurysm (*arrows*)

of central low-grade cartilaginous tumours, therefore supporting the theory that enchondromas represent neoplasms [39].

The true prevalence of enchondroma is unknown since many lesions are asymptomatic [40, 41]. However, in a series of 3,067 primary bone tumours and tumour-like lesions, enchondroma accounted for 237 lesions (19.7% of cartilage tumours and 7.7% of all cases) [34]. Furthermore, a retrospective study of 449 routine MR examinations of the knee identified that the prevalence of incidental enchondromas on routine MRI of the knee was 2.9% with the distal femur being most commonly involved with a prevalence of 2% [42].

Enchondromas usually present in the 3rd to 4th decade, typically as incidental findings on radiographs or MRI studies performed for other reasons [40, 41]. For example, symptoms in patients identified as having a solitary enchondroma of the proximal humerus have been found to be due to alternative pathology in approximately 80% of cases, typically related to rotator cuff disease [41]. However, a rarely reported cause of rotator cuff impingement includes an enchondroma of the acromion [43]. Pathological fracture is a well-recognised presentation of tumours of the small bones of the hand, particularly of the little finger, in which case low-grade chondral tumours are by far the commonest cause [44].

With regards location, 40–65% of enchondromas are found in the small bones of the hand, of which 40–50% are in the proximal phalanx, 15–30% in the metacarpals and 20–30% in the middle phalanges [36]. The little finger is most commonly involved and the thumb least. Approximately 25% of chondromas involve the major long bones, most commonly the femur, followed by the humerus and tibia. Approximately 7% of all cases involve the small bones of the feet [36]. All other sites are rare.

Enchondromas can be managed either by careful clinical and radiological observation, or by intralesional curettage [35], in which case local recurrence is very rare.

Chondromas are classically intramedullary lesions of the long bone metaphysis, but lesions have also been described in an epiphyseal location [45], within the cortex [46] and on the surface of the bone, when they are referred to as juxtacortical or periosteal chondromas (see later) [47–49]. Approximately 8% of long bone chondromas are centred in the epiphysis [45], although the majority extend either into the metaphysis and/or the sub-chondral bone. The proximal humerus and distal femur are the commonest sites of primary epiphyseal lesions.

Rarely, cases have also been reported in the rib [50], radius [51], little toe [52], clavicle [53] and cuboid bone [54]. Cases of combined enchondroma and periosteal chondroma mimicking chondrosarcoma have also been described [55, 56]. The carpus is another rare site of occurrence for chondromas. A review of carpal bone cysts treated at a single specialist institution over 10 years yielded only 3 cases [57].

Enchondroma protuberans describes an unusual form of the lesion, which arises in the medullary cavity, but has an exophytic growth pattern [58]. It is most commonly located in the phalanges and metacarpals, but has also been reported in the ribs and humerus.

Enchondromas arising in the hand are typically centrally located in the diaphysis, but may extend to the end of the smaller tubular bones [34, 36]. The tumour is classically lobular in contour and associated with endosteal scalloping, which is commonly deep and associated with cortical

thinning and a variable degree of bone expansion. However, cortical breakthrough and periostitis are not expected unless there has been a pathological fracture (Fig. 10). Chondroid matrix mineralization is seen in the majority of lesions (Fig. 10).

Long bone enchondromas are usually located centrally or eccentrically in the diaphysis or metaphysis, in the latter situation occasionally associated with epiphyseal extension [34, 36]. The lesion margin is non-sclerotic and therefore, in the absence of much matrix mineralization, the intramedullary extent of the tumour may be poorly appreciated on radiography (Fig. 11). A minor degree of endosteal scalloping, cortical thinning and bone expansion may be evident (Fig. 12a, b). Approximately 95% of cases will show some degree of matrix mineralization (Figs. 11a, 12a). The lesion is usually less than 6 cm in maximal length.

Computed tomography may show additional features such as radiographically occult matrix mineralization and endosteal scalloping, while the MRI features are classical [34, 36]. The tumour is typically lobular in contour with intermediate T1W and high T2W signal intensity consistent with hyaline cartilage (Figs. 11b, 12b, 13, 14). Small regions of increased T1W SI may be present owing to engulfed normal medullary fat (Fig. 13a), while thin hypointense septa are commonly seen between lobules of cartilage on T2W images. Such fibrovascular septa show enhancement following gadolinium (Fig. 14b). Matrix mineralization appears as punctate or curvilinear areas of signal void (Figs. 11b, 13a, 14a).

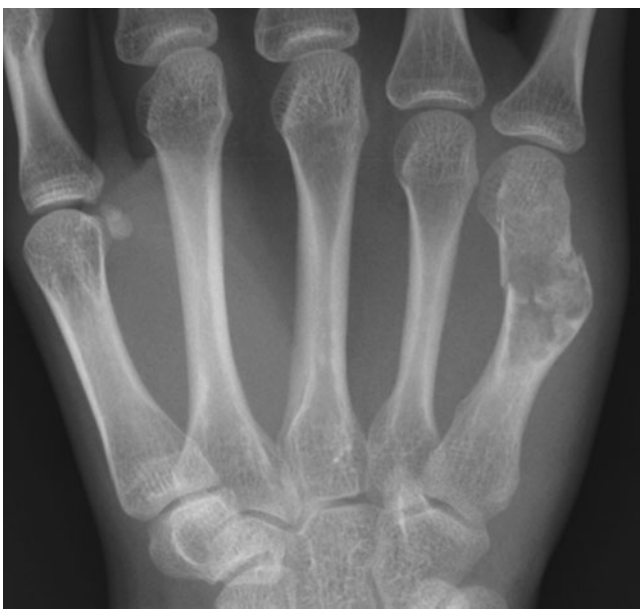

Fig. 10 Enchondroma of the little finger metacarpal. Anteroposterior radiograph shows a pathological fracture through an expansile lesion with associated chondral-type matrix mineralisation

Lesions show mild/moderate uptake on 99^{m}-Tc MDP bone scintigraphy, which is usually less than or equal to that seen in the anterior iliac crest [36]. Increased activity on FDG PET studies has also been reported [59].

Epiphyseal chondromas differ slightly in that they typically show a thin sclerotic margin [34, 36, 45]. They have a mean size of 2.7 cm with a range of 1.1 to 4.9 cm [45]. The absence of any reactive change will help to differentiate them from chondroblastoma (Fig. 15).

Enchondroma protuberans has a different radiological appearance [58]. The lesion is located centrally or eccentrically within the bone and is associated with extension through the cortex to form a lobular extraosseous mass, which may be partially surrounded by a thin calcified rim (Fig. 16). The MR signal characteristics are as for enchondroma, and MRI clearly demonstrates the continuity between the intramedullary and extraosseous components.

Enchondroma vs low-grade chondrosarcoma

The differentiation between enchondroma and low-grade chondrosarcoma (CS) has been studied extensively [60–63]. The difficulty in the differentiation of enchondromas from low-grade CS and the difficulty in the histological grading of CS have been emphasized in two recent studies that evaluated the interobserver variability in the diagnosis and histological grading of cartilaginous tumours [64, 65]. Both studies found low reliability in the distinction between enchondromas and low-grade CS as well as low reliability in the histological grading of CS amongst bone tumour pathologists [64, 65]. Furthermore, the SLICED study group also demonstrated significant variation between radiologists in differentiating enchondromas from low-grade CS as well as low reliability in the grading of CS based on radiography or CT, with slightly improved agreement amongst radiologists when MRI was used [64]. Therefore, in our institution, the differentiation of benign from low-grade malignant cartilage tumours is made in a multi-disciplinary team and based on clinical, imaging and pathology findings. Despite the radiological and pathological challenges in the differentiation of enchondromas from low-grade CS, the two lesions may be treated with the same management strategy.

With regards location, enchondromas most commonly arise in the small bones of the hands and feet, while CS is exceedingly rare in these sites. Alternatively, CS is relatively common in the pelvic bones while enchondroma is rare. The major difficulty lies, therefore, in the differentiation between enchondroma and low-grade CS in the major long bones.

Murphey et al. looked at statistically significant differentiating features between enchondroma and CS in the appendicular skeleton, excluding cases arising in the hands and feet. Clinical features that significantly favour CS included

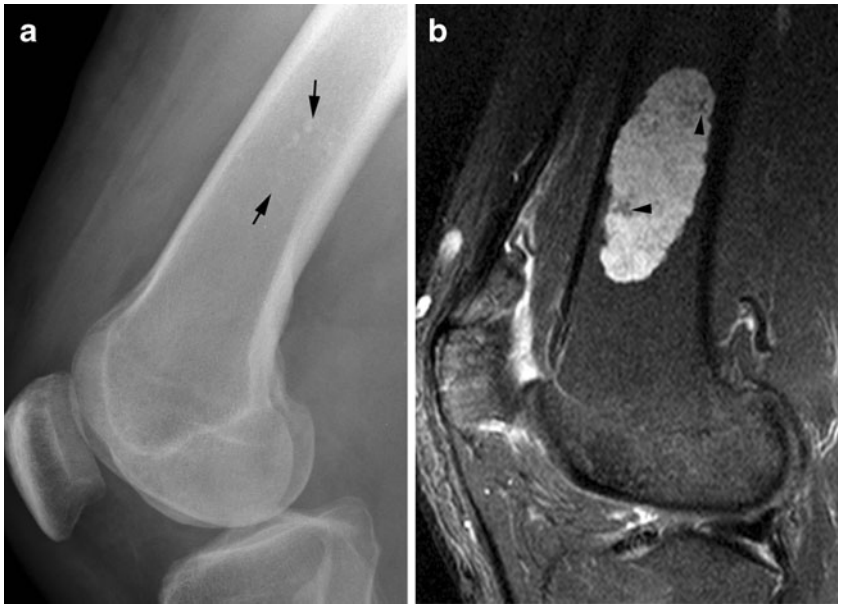

Fig. 11 Chondroma of the distal femoral metadiaphysis. **a** Lateral radiograph demonstrates a lytic lesion with a minor degree of chondral-type matrix mineralisation (*arrows*). **b** Sagittal STIR MR image shows the lesion to be much more extensive than suggested on the plain radiograph, with heterogeneous increased SI and punctate areas of hypointensity due to matrix mineralisation (*arrowheads*)

male sex, older age at presentation (mean age 50 years), and the presence of pain (in 95% of cases). Both lesions most commonly arose in the femur, although enchondroma was more common distally and CS in the proximal femur. Within individual bones, CS was more commonly centred in the epiphysis or metaphysis, while enchondroma was commoner in the diaphysis. CS was also greater in size than enchondroma (mean size on CT/MRI being 8 cm vs 5 cm). Depth and extent of endosteal scalloping was greater for CS, with more than two thirds of the depth of the cortex involved in ~90% of cases as shown by CT or MRI. Other features that were commoner with CS included cortical remodelling, cortical destruction, pathological fracture, periosteal reaction and soft tissue extension [61]. A study by Bui et al., however, evaluated the cross-sectional imaging of 11 eccentric enchondromas of long bone that were smaller than 4 cm for the prevalence and extent of cortical scalloping. They found that the prevalence of cortical scalloping in eccentric enchondroma was 100% and that 8 out of 11 eccentric enchondromas demonstrated endosteal scalloping of more than two thirds whilst 3 lesions demonstrated outer cortical penetration. They therefore concluded that in this small subgroup of chondroid lesions, the degree of cortical scalloping was due to lesion location and not a sign of malignancy. Furthermore, they postulated that eccentric enchondroma originated from the endosteum and termed the lesion "endosteal chondroma" [66].

With regard to lesions located specifically in the fibula, features that favour low-grade CS include soft-tissue mass, periosteal reaction, cortical disruption in the juxta-articular fibula, cortical thickening, and tumour size greater than 4 cm [67].

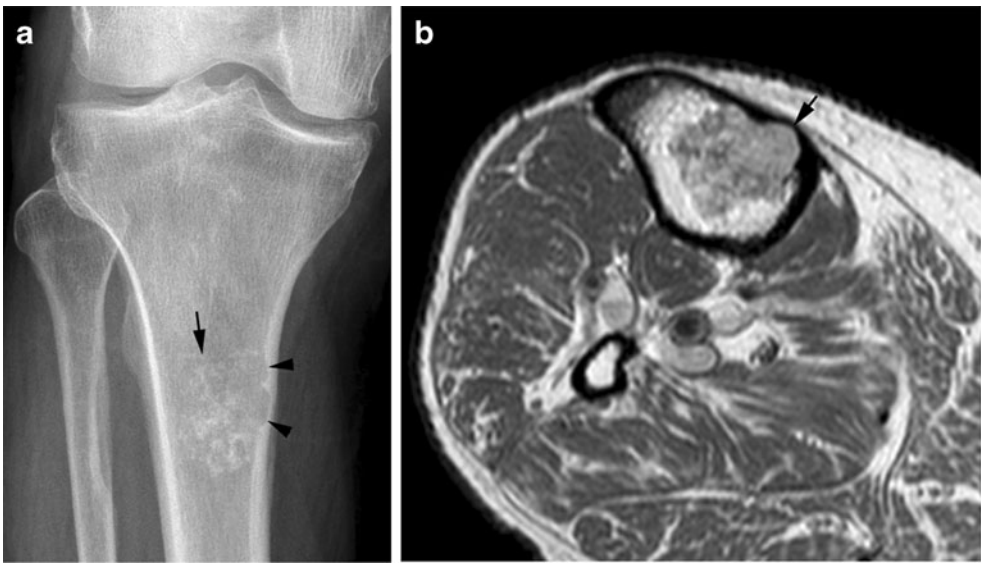

Fig. 12 Chondroma of the proximal tibial metadiaphysis. **a** Anteroposterior radiograph demonstrates a lobular lytic lesion with a thin sclerotic margin (*arrow*), a moderate degree of chondral-type matrix mineralisation and deep endosteal scalloping (*arrowhead*). **b** Axial PDW FSE MR image shows the lesion to have heterogeneous increased SI between that of muscle and medullary fat. Note the deep endosteal scalloping (*arrow*)

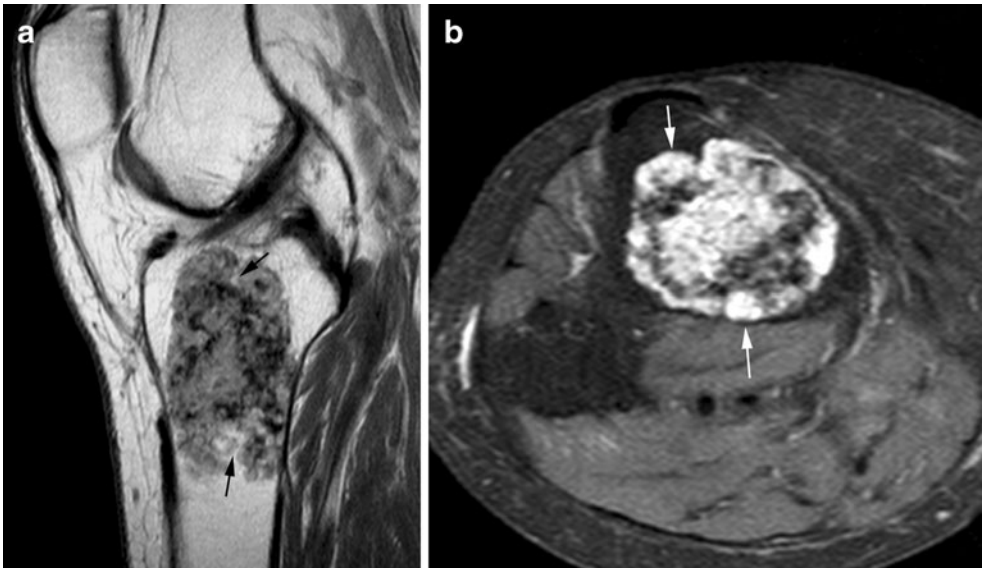

Fig. 13 Chondroma of the proximal tibial metaphysis. **a** Sagittal T1W SE MR image shows a heterogeneous intermediate SI lesion with punctate areas of hypointensity due to matrix mineralisation and some areas of trapped medullary fat (*arrows*). **b** Axial STIR image shows the lesion to have heterogeneous increased SI (*arrows*). Note the absence of any reactive medullary or soft tissue change

In the foot, a lesion size greater than 5 cm and location in the mid- or hind-foot favour CS [68].

Periosteal chondroma

Periosteal chondroma is a rare benign tumour arising on the surface of the cortex, but deep to the periosteum. It typically presents in the 3rd to 4th decades of life with a painful swelling, most often related to the metaphyseal ends of long bones and the small bones of the hands and feet. Based on a review of 3 series totalling 55 cases, the following sites were involved; humerus (n=18), femur (n=11), tibia (n=4), phalanges (n=9), radius (n=2) and ulna (n=1) [47–49]. Individual cases have also been reported in the rib [50], clavicle [53] and cuboid [54]. The finding of concurrent periosteal chondroma and enchondroma may mimic chondrosarcoma [55, 56].

Radiological features include cortical scalloping with/without sclerosis, a thin periosteal shell (Fig. 17), chondroid matrix mineralisation (Figs. 17, 18) and rarely intramedullary invasion [47, 48]. Minor elevation of the bony cortex at the margins of the lesion is also a feature (Fig. 18a). Mean lesion size is 2.2–2.6 cm (range 1–7 cm) [48, 49]. This differs significantly from periosteal chondrosarcoma, which has a mean size of 5.5 cm (range 3–14 cm) [48].

Magnetic resonance imaging features include a lobular contour, with the tumour showing typical SI characteristics of chondral tissue, intermediate on T1W SE and hyperintense on T2W FSE sequences (Fig. 18b). A thin outer hypointense lining is noticeable on T2*W GE images in particular [48, 49]. Following contrast medium administration, thin peripheral and septal enhancement may be observed. Perilesional or intramedullary reactive oedema is a rare feature.

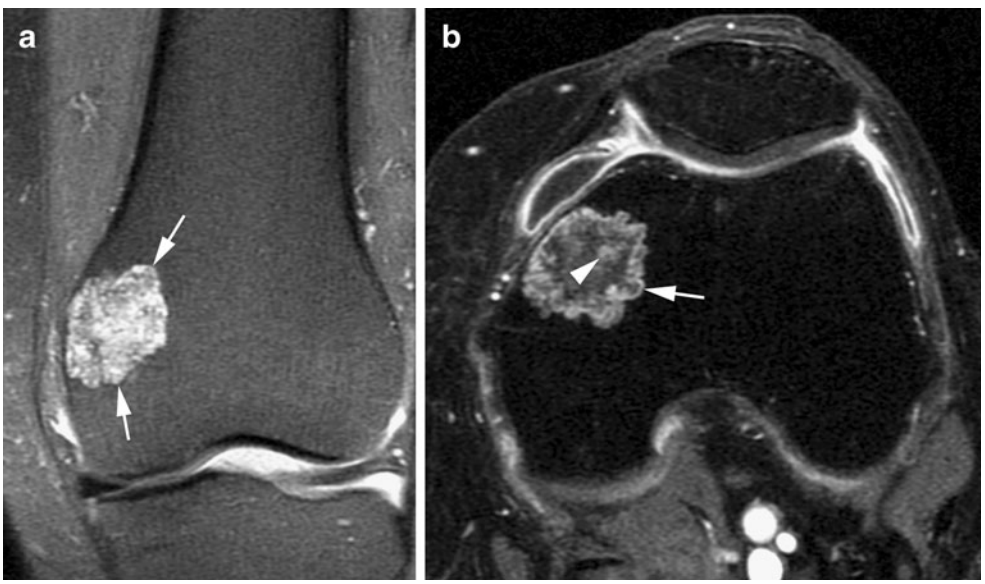

Fig. 14 Chondroma of the distal femoral epiphysis and metaphysis. **a** Coronal PDW FSE FS MR image shows a lobular, heterogeneous hyperintense lesion (*arrows*) with punctate areas of hypointensity due to matrix mineralisation. Note the absence of reactive medullary oedema-like SI. **b** Axial post-contrast T1W SE FS MR image shows a combination of peripheral (*arrow*) and central nodular enhancement (*arrowhead*)

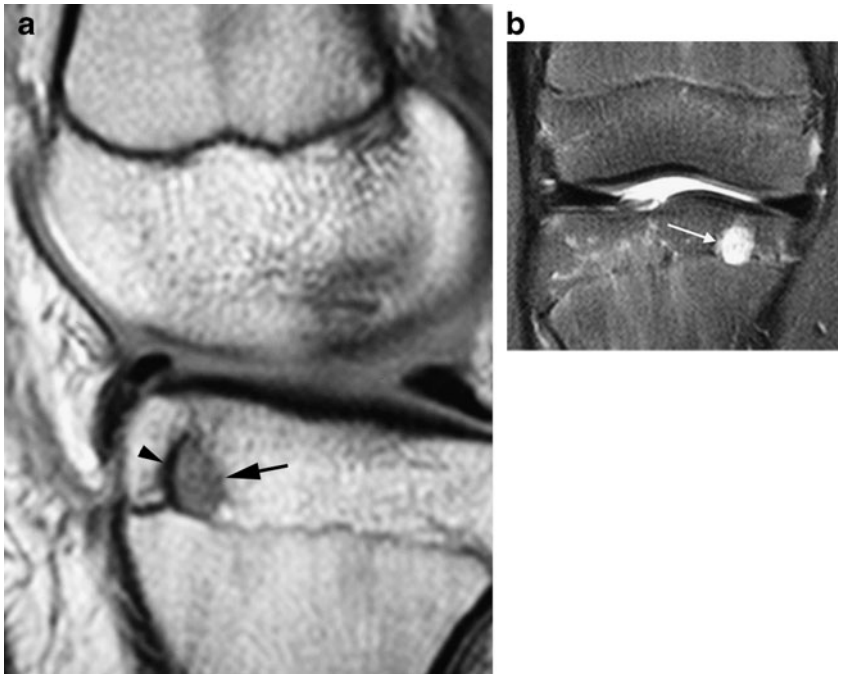

Fig. 15 Chondroma of the proximal tibial epiphysis. **a** Sagittal PDW FSE and **b** coronal T2W SE FS MR images show a small heterogeneous lesion (*arrow*) in the anterior aspect of the epiphysis. Note the absence of reactive medullary oedema-like SI on the T2W SE FS MRI and the presence of chemical shift artefact on the PDW MRI (*arrowhead*), features that help to distinguish the lesion from a chondroblastoma

Chondroblastoma

Chondroblastoma (CB) is a rare benign chondral tumour characterised by an epiphyseal location in long bones. It is estimated to represent <1% of all primary bone tumours, although it accounted for 4.7% of cases reviewed at the Mayo Clinic over a 5-year period [69]. Based on the review of a total of 540 cases from a combination of four large surgical and pathological series [70–73], the mean age at presentation was 19.9 years with a range of 8–69 years and a male:female ratio of 2.7:1.

Clinical presentation is typically with pain (98%), local tenderness (90%), stiffness (74%) and swelling (40%), while joint effusion is present in 4% [71]. Approximately 75–80% of all cases involve the long bones [73], with the following distribution determined by review of a combination of 541

Fig. 16 Enchondroma protuberans of the 4th toe proximal phalanx. Anteroposterior radiograph of the forefoot showing an eccentrically placed lesion (*arrowhead*) in the proximal shaft that has extended through the lateral cortex (*arrow*)

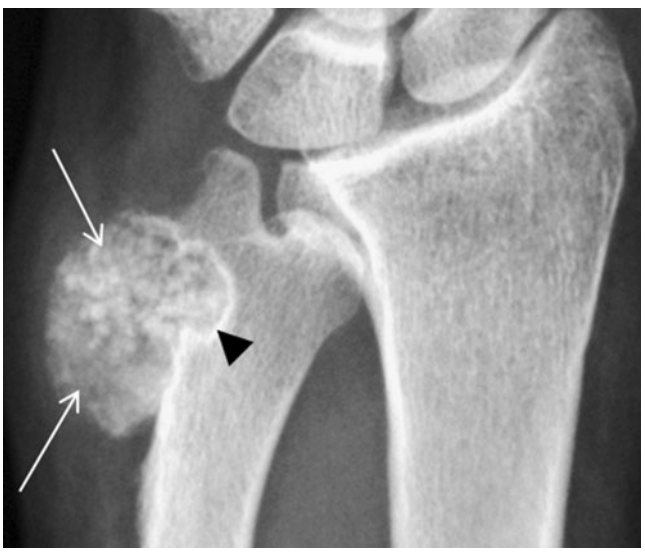

Fig. 17 Periosteal chondroma of the distal ulna. Anteroposterior radiograph shows a heavily mineralised surface lesion (*white arrows*) with associated cortical scalloping (*black arrowhead*) and an outer cortical shell

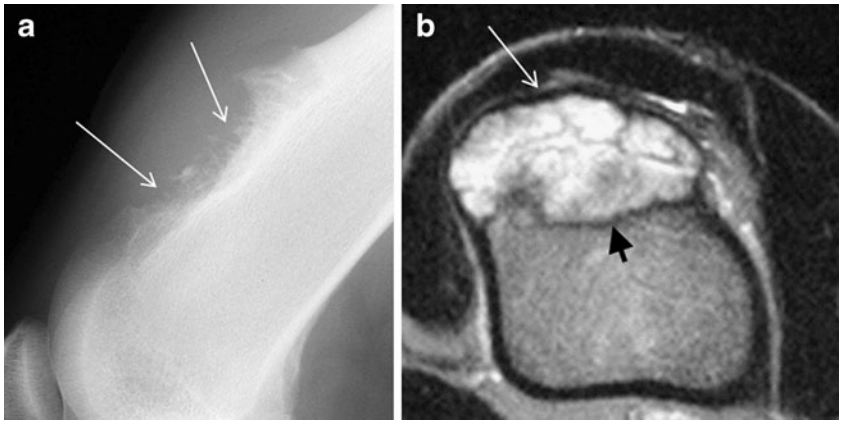

Fig. 18 Periosteal chondroma of the distal femur. **a** Lateral radiograph shows a large mineralised anterior surface lesion (*arrows*) with cortical scalloping. **b** Axial T2W FSE FS MR image shows a lobular lesion with typical SI characteristics of a low-grade chondral tumour, a thin hypointense peripheral margin (*long white arrow*) due to the overlying intact periosteum and the intact femoral cortex (*small black arrow*)

long bone cases from the literature [70–75]; proximal tibia 137 (25.3%), distal femur 130 (24.0%), proximal humerus 122 (22.6%), proximal femur 119 (22%), distal tibia 20 (3.7%), distal humerus 7 (1.4%), fibula 3 (0.6%) and radius/ulna 3 (0.6%). Over 90% of long bone cases involve the epiphysis or apophysis, with extension into the adjacent metaphysis being relatively common with closure of the growth plate.

After the long bones, the foot is the second commonest site of occurrence, with approximately 12% located in this region [69, 73], most commonly in the talus (44%) and calcaneus (39.1%), and occasionally in the cuboid (8%). CB of the foot is more commonly seen in male subjects (81%) and at a mean age of 25.5 years, which is significantly older than for long bone CB [69].

Chondroblastoma is typically treated with intralesional curettage and packing of the defect with bone graft or cement. Such management, when adequately performed, is associated with an excellent outcome. Of 242 cases [70–72, 75], a single local recurrence occurred in 24 patients (10%), with some cases showing multiple local recurrences. Malignant transformation is a risk of multiple recurrences, occurring in 6 cases (2.5%) with 7 patients (2.9%) developing lung metastases. A total of 5 patients (2%) died of their disease. More recently, successful treatment with CT-guided radiofrequency (RF) ablation has been described [76].

Unusual lesion site can be related to rare locations within commonly affected bones or rarely involved skeletal locations. Purely metaphyseal and/or diaphyseal CB is very rare. Recently, a retrospective study of 390 cases of CB identified 7 cases of CB (1.8%) that were located entirely in the metaphysis and/or diaphysis [77]. Intracortical CB has also been reported [78]. CB has also been described in the scapula [79], the acromion [80], the rib [81], the tri-radiate cartilage [82], the sacrum [83] and within the small bones of the hands and feet [69]. In a study by Singh et al. who reviewed 59 lesions of the patella, 15% of all lesions (9 cases) were CB [84].

Atypical aggressive behaviour at primary presentation is also recorded, including extraosseous extension of a large

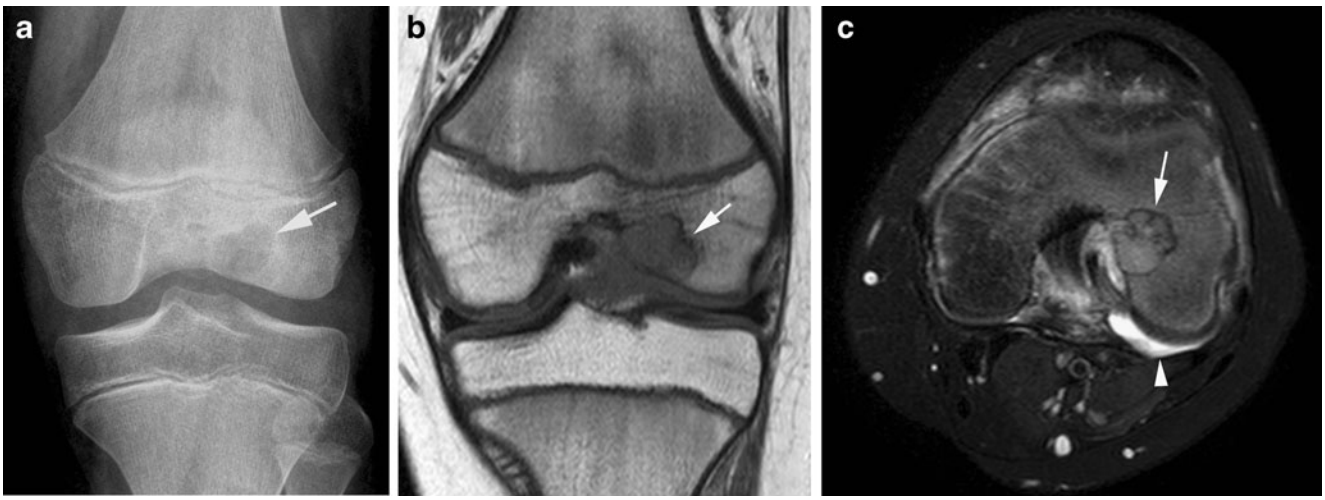

Fig. 19 Chondroblastoma of the distal femoral epiphysis. **a** Anteroposterior radiograph demonstrates a well-defined lobular lytic lesion with a thin sclerotic margin (*arrow*). **b** Coronal T1W SE MR image shows a homogeneous intermediate SI lesion (*arrow*). **c** Axial PDW FSE FS MR image shows an intermediate SI lesion (*arrow*) with associated marrow oedema and reactive joint effusion (*arrowhead*)

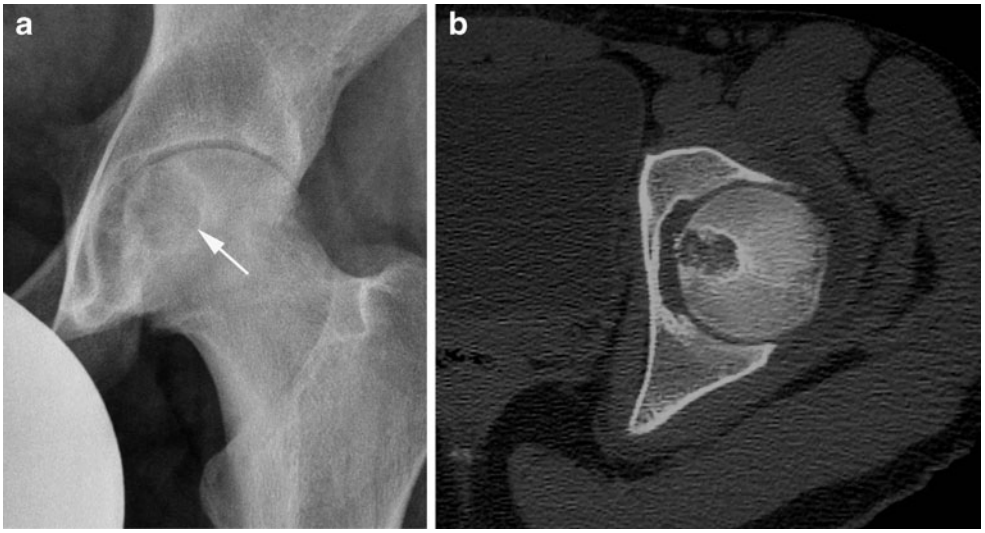

Fig. 20 Chondroblastoma of the proximal femoral epiphysis. **a** Anteroposterior radiograph demonstrates a well-defined lobular lytic lesion with a thin sclerotic margin (*arrow*). **b** Axial CT study shows subtle matrix mineralisation

humeral lesion requiring forequarter amputation [85], extension of a tibial CB into the knee joint [86] and aggressive scapular CB associated with pulmonary metastases [79]. Metastases from CB may also be benign [87].

Radiography of CB classically demonstrates a 1- to 4-cm lesion with a thin, sclerotic, geographic margin, a lobular contour and matrix mineralisation in approximately 30% of cases radiographically (Figs. 19, 20, 21) [88]. The tumour is classically located adjacent to the growth plate with almost half the cases limited to the epiphysis, but the majority extending for a variable degree into the metaphysis (Figs. 22, 23) [88]. As mentioned previously purely metaphyseal and/or diaphyseal chondroblastomas are exceedingly rare, representing only 1.8% of all CB in a recent study (Fig. 24) [77]. A thick, solid periosteal reaction is present in almost 60% of long bone CB, occurring in the metaphysis adjacent to the epiphyseal lesion (Fig. 23) [89]. The presence of periostitis may help differentiate between CB and other lytic epiphyseal lesions. Tumours arising in the foot have similar characteristics [74, 75], but in addition commonly result in bone expansion (Fig. 25) [88].

Scintigraphy demonstrates uptake on vascular and delayed phases [90], while there is a single report of positive PET [91]. CT may demonstrate features such as extraosseous extension, sclerotic margin and matrix mineralisation that are not appreciated radiographically (Fig. 20b) [92].

The MRI features of CB have been extensively studied [93–97]. The lesion typically demonstrates intermediate T1W SI (Fig. 19b) and in the majority of cases, either complete or partial T2W hypointensity, which is related histologically to abundant immature chondral matrix, hypercellularity of chondroblasts, calcifications and haemosiderin (Fig. 22b). A lobular, thin hypointense margin is seen (Figs.19b, c, 22b) and the vast majority of cases (>90%) show marked peri-lesional oedema-like marrow SI (Figs. 19c, 22b). Periostitis, soft tissue oedema, reactive joint effusion and synovitis are also commonly seen (Figs. 19c, 23). ABC change is reported in approximately 15% of cases [88] and manifests on MRI as regions of fluid SI [97] and fluid–fluid levels (Fig. 26). Following contrast medium administration, either lobular or peripheral/septal enhancement is visualised in all cases [96, 97].

Magnetic resonance imaging may be useful in the assessment of possible recurrence, with histologically proven recurrent lesions demonstrating marrow oedema [94], while absence of recurrence is associated with resolution of reactive marrow and soft tissue changes [94, 95].

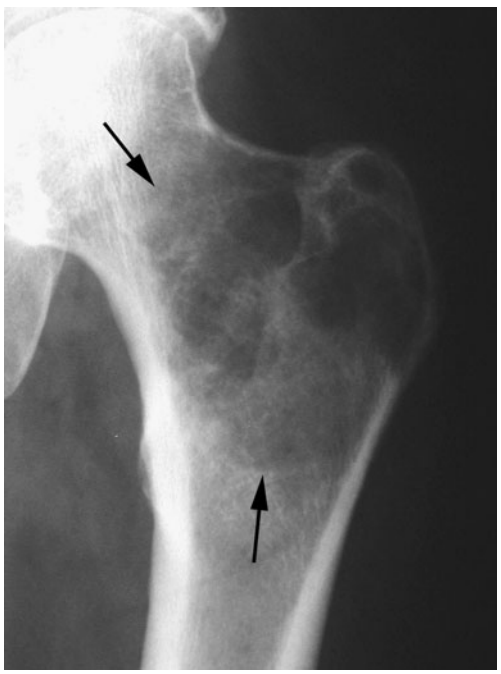

Fig. 21 Non-epiphyseal chondroblastoma of the proximal femur. Anteroposterior radiograph demonstrates a large, poorly defined lytic lesion with a non-sclerotic margin in the femoral neck and greater trochanter

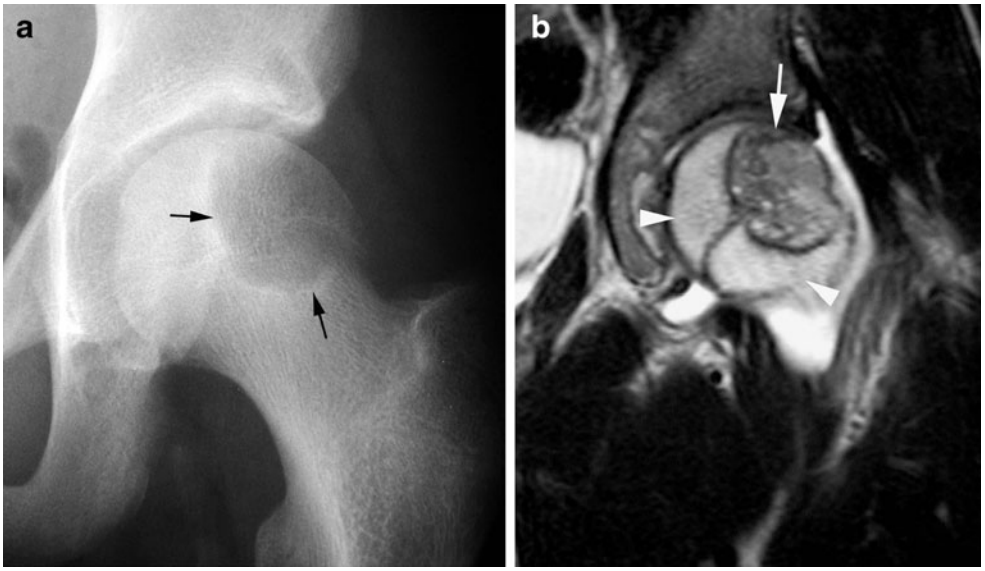

Fig. 22 Chondroblastoma of the proximal femur. **a** Anteroposterior radiograph demonstrates a well-defined lytic lesion with a thin sclerotic margin (*arrows*) crossing the physis. **b** Coronal STIR MR image shows the lesion to have intermediate SI (*arrow*) and demonstrate extensive epiphyseal and metaphyseal marrow oedema (*arrowheads*) and a joint effusion

Chondromyxoid fibroma

Chondromyxoid fibroma (CMF) is a very rare lesion accounting for significantly less than 1% of all primary bone neoplasms. In a review of over 10,000 primary benign and malignant bone tumours, CMF accounted for approximately 40 cases (0.004%) [98]. From a total of 171 cases reported in five separate studies [98–102], 96 occurred in male subjects and 75 in female (M:F ratio of 1.28:1), with a mean age at presentation of 25.1 years and an age range of 3–70 years.

The tumour may arise in a variety of locations, but most commonly involves the medullary cavity of the lower limb long bones (~65%). A combination of 111 long bone cases from 5 series [98–102] identified 52 (46.8%) in the tibia (47 proximal and 5 distal), 32 (28.8%) in the femur (9 proximal and 23 distal), 18 (16.2%) in the fibula (10 proximal and 8 distal), 7 (6.3%) in the ulna/radius and only 2 (1.8%) in the humerus. Therefore, less than one third of all lesions involve the tibia.

Approximately 20% of cases involving the appendicular skeleton arise in the foot, most commonly the phalanges and metatarsals [103], while 10% involve the pelvic girdle (most

Fig. 23 Chondroblastoma of the proximal tibia. Anteroposterior radiograph demonstrates a large lesion with a non-sclerotic margin (*black arrows*). Solid periosteal reaction is also evident in the adjacent metaphysis (*white arrow*)

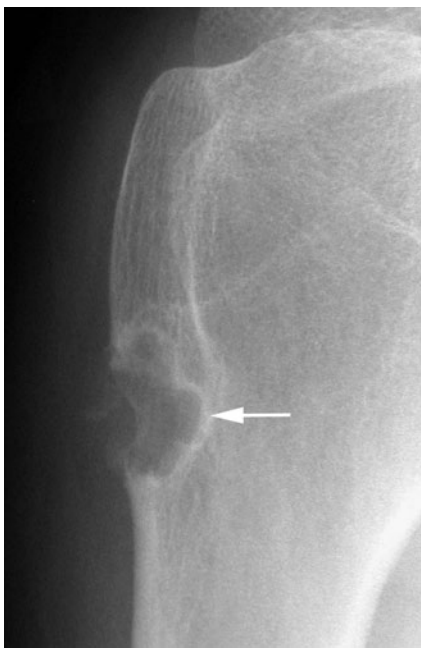

Fig. 24 Metaphyseal chondroblastoma of the proximal humerus. Anteroposterior radiograph demonstrates a small lytic lesion with a sclerotic margin (*arrow*) in the proximal metaphysis

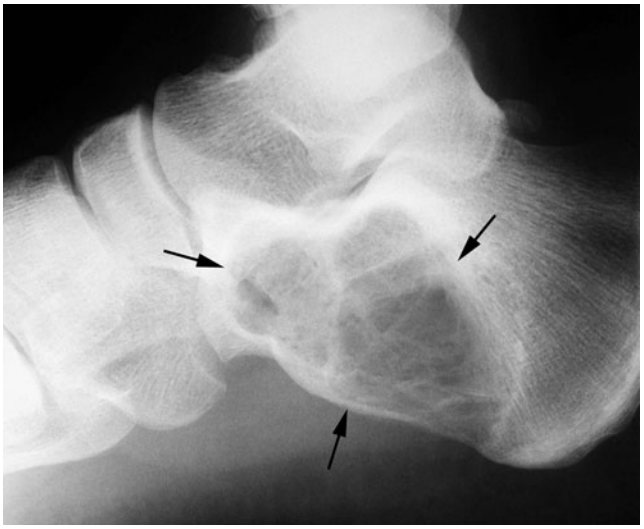

Fig. 25 Chondroblastoma of the calcaneus. Lateral radiograph demonstrates a large lytic lesion (*arrows*) with internal trabeculation

commonly the iliac blade) and 5% are located in the small bones of the hand.

As stated, the lesion typically arises within the medullary cavity. However, CMF has also been reported to occur in an intracortical [104], sub-periosteal [105] and juxta-cortical [106] location, the latter accounting for ~5% of cases. Rarely reported locations include the ribs [101], sternum [107], scapula [108], acromion [109], clavicle [110] and sacrum [111]. Rare occurrence of extraosseous growth of a primary intramedullary lesion has been described [109].

Within the long bones, CMF is centred in the metaphyseal region in just over 50% of cases and in a predominantly

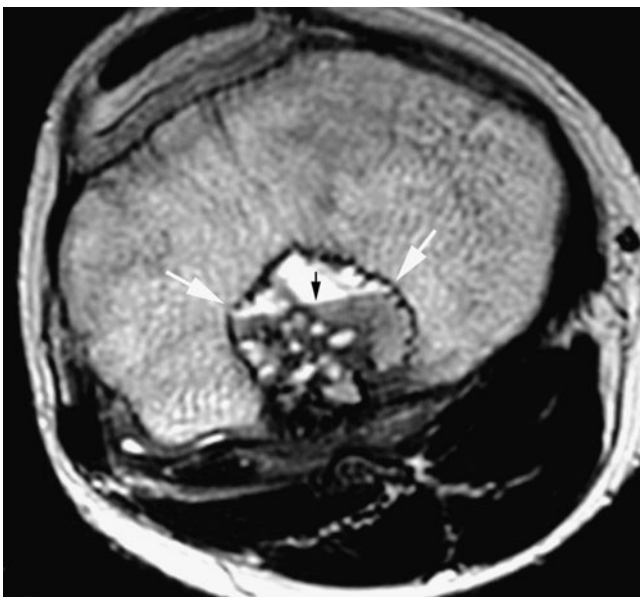

Fig. 26 Chondroblastoma of the proximal tibia. Axial T2W FSE MR image shows the lesion to have multiple fluid levels (*black arrow*) and a thin hypointense margin (*white arrows*)

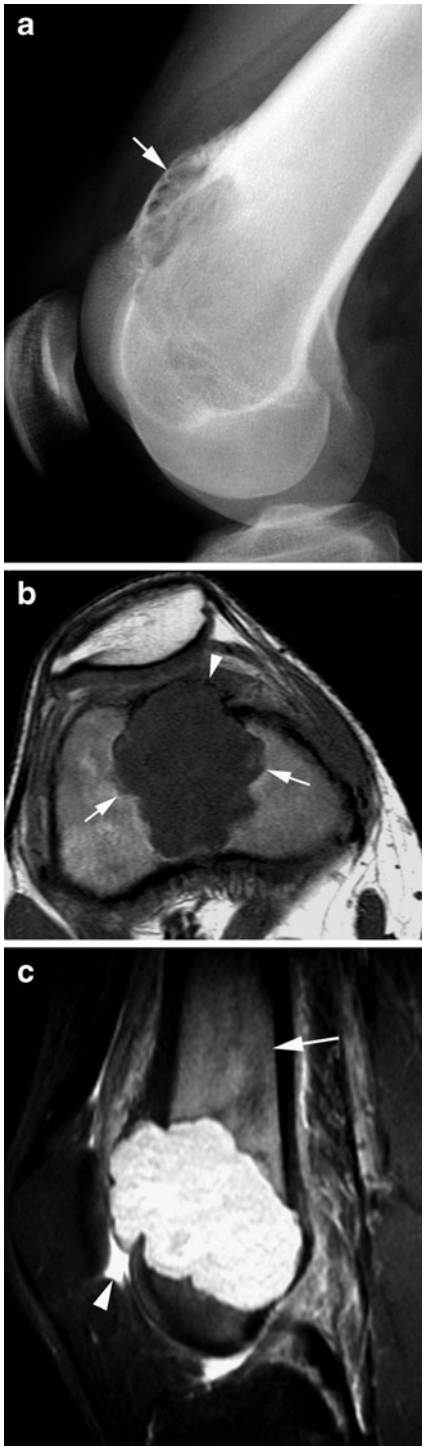

Fig. 27 Chondromyxoid fibroma of the distal femur. **a** Lateral radiograph demonstrates a metaphyseal and epiphyseal lytic lesion with a thin sclerotic border and extension through the anterior cortex (*arrow*). **b** Axial T1W SE MR image shows the lesion to have a lobular contour (*arrows*) with extension through the anterior cortex (*arrowhead*) and intermediate SI. **c** Sagittal STIR MR image shows a lesion with heterogeneous increased SI, extensive reactive medullary oedema (*white arrow*) and a small reactive joint effusion (*white arrowhead*)

diaphyseal location in approximately 40% of cases [100, 101]. Epiphyseal CMF is described, but is very rare. Almost all lesions are intramedullary, being situated eccentrically in approximately 60% of cases (Fig. 27) and centrally in the remainder. A geographic pattern of bone destruction with a well-defined, sclerotic rim and commonly a round or elongated, lobular border is the classic appearance. Cortical thinning and expansion are also very common features, and complete cortical destruction may be seen in almost one third of cases. Internal trabeculation is present in two thirds of patients, but radiographically evident matrix mineralisation is uncommon, being reported in approximately 2–15% of lesions. Similar findings are described in non-long bone locations.

The MRI features have been rarely reported and are non-specific (Fig. 27b, c) [110, 111].

Conclusion

Benign cartilage tumours represent a broad spectrum of neoplasms, ranging from the frequently observed and often incidentally diagnosed osteochondroma to the exceedingly rare chondromyxoid fibroma. Radiography remains the mainstay in the initial work-up of benign cartilage lesions. However cross-sectional imaging, in particular MRI, is of superior accuracy in the characterisation and diagnosis of benign cartilage lesions and in the assessment of potential complications. Thus, MRI leads to increased diagnostic confidence in the assessment of benign cartilage neoplasms, thereby avoiding the need for biopsy in a large majority of patients.

Conflicts of interest The authors declare that they have no conflict of interest.

References

1. Brien EW, Mirra JM, Luck Jr JV. Benign and malignant cartilage tumors of bone and joint: their anatomic and theoretical basis with an emphasis on radiology, pathology and clinical biology. II. Juxtacortical cartilage tumors. Skeletal Radiol. 1999;28:1–20.
2. Murphey MD, Choi JJ, Kransdorf MJ, Flemming DJ, Gannon FH. Imaging of osteochondroma: variants and complications with radiologic–pathologic correlation. Radiographics. 2000;20:1407–34.
3. Saglik Y, Altay M, Unal VS, Basarir K, Yildiz Y. Manifestations and management of osteochondromas: a retrospective analysis of 382 patients. Acta Orthop Belg. 2006;72:748–55.
4. Hameetman L, Szuhai K, Yavas A, Knijnenburg J, van Duin M, van Dekken H, et al. The role of EXT1 in nonhereditary osteochondroma: identification of homozygous deletions. J Natl Cancer Inst. 2007;99:396–406.
5. Bovee JV, Hogendoorn PC, Wunder JS, Alman BA. Cartilage tumours and bone development: molecular pathology and possible therapeutic targets. Nat Rev Cancer. 2010;10:481–8.
6. Garcia RA, Inwards CY, Unni KK. Benign bone tumors—recent developments. Semin Diagn Pathol. 2011;28:73–85.
7. Taitz J, Cohn RJ, White L, Russell SJ, Vowels MR. Osteochondroma after total body irradiation: an age-related complication. Pediatr Blood Cancer. 2004;42:225–9.
8. Bordigoni P, Turello R, Clement L, Lascombes P, Leheup B, Galloy MA, et al. Osteochondroma after pediatric hematopoietic stem cell transplantation: report of eight cases. Bone Marrow Transplant. 2002;29:611–4.
9. Faraci M, Bagnasco F, Corti P, Messina C, Fagioli F, Podda M, et al. Osteochondroma after hematopoietic stem cell transplantation in childhood. An Italian study on behalf of the AIEOP-HSCT group. Biol Blood Marrow Transplant. 2009;15:1271–6.
10. De Smet L, Degreef I. Bilateral osteochondroma of the scaphoid causing scapholunate dissociation: a case report. Chir Main. 2007;26:141–2.
11. Takagi T, Matsumura T, Shiraishi T. Lunate osteochondroma: a case report. J Hand Surg Am. 2005;30:693–5.
12. Nogier A, De Pinieux G, Hottya G, Anract P. Case reports: enlargement of a calcaneal osteochondroma after skeletal maturity. Clin Orthop Relat Res. 2006;447:260–6.
13. Joshi D, Kumar N, Singh D, Lal Y, Singh AK. Osteochondroma of the talus in a male adolescent. J Am Podiatr Med Assoc. 2005;95:494–6.
14. Lee SK, Jung MS, Lee YH, Gong HS, Kim JK, Baek GH. Two distinctive subungual pathologies: subungual exostosis and subungual osteochondroma. Foot Ankle Int. 2007;28:595–601.
15. Bozkurt M, Dogan M, Turanli S. Osteochondroma leading to proximal tibiofibular synostosis as a cause of persistent ankle pain and lateral knee pain: a case report. Knee Surg Sports Traumatol Arthrosc. 2004;12:152–4.
16. Carpintero P, Leon F, Zafra M, Montero M, Berral FJ. Fractures of osteochondroma during physical exercise. Am J Sports Med. 2003;31:1003–6.
17. Mohsen MS, Moosa NK, Kumar P. Osteochondroma of the scapula associated with winging and large bursa formation. Med Princ Pract. 2006;15:387–90.
18. Kirkos JM, Papavasiliou KA, Kyrkos MJ, Kapetanos GA. Bursal osteochondromatosis overlaying an osteochondroma in the immature skeleton. J Pediatr Orthop B. 2007;16:160–3.
19. Guy NJ, Shetty AA, Gibb PA. Popliteal artery entrapment syndrome: an unusual presentation of a fibular osteochondroma. Knee. 2004;11:497–9.
20. Argin M, Biceroglu S, Arkun R, Parildar M. Solitary osteochondroma causing popliteal pseudoaneurysm that presented as a mass lesion. Diagn Interv Radiol. 2007;13:190–2.
21. Blazick E, Keeling WB, Armstrong P, Letson D, Back M. Pseudoaneurysm of the superficial femoral artery associated with osteochondroma—a case report. Vasc Endovascular Surg. 2005;39:355–8.
22. Turan Ilica A, Yasar E, Tuba Sanal H, Duran C, Guvenc I. Sciatic nerve compression due to femoral neck osteochondroma: MDCT and MR findings. Clin Rheumatol. 2008;27:403–4.
23. Gray KV, Robinson J, Bernstein RM, Otsuka NY. Splitting of the common peroneal nerve by an osteochondroma: two case reports. J Pediatr Orthop B. 2004;13:281–3.
24. Kim JY, Ihn YK, Kim JS, Chun KA, Sung MS, Cho KH. Nontraumatic peroneal nerve palsy: MRI findings. Clin Radiol. 2007;62:58–64.
25. Reichmister J, Reeder JD, Gold DL. Osteochondroma of the distal clavicle: an unusual cause of rotator cuff impingement. Am J Orthop (Belle Mead NJ). 2000;29:807–9.

26. Reize F, Buess E. Humeral osteochondroma causing a subscapularis tear: a rare source of shoulder dysfunction. Arch Orthop Trauma Surg. 2007;127:67–70.
27. Onga T, Yamamoto T, Akisue T, Marui T, Kurosaka M. Biceps tendinitis caused by an osteochondroma in the bicipital groove: a rare cause of shoulder pain in a baseball player. Clin Orthop Relat Res. 2005:241–244.
28. Lamovec J, Spiler M, Jevtic V. Osteosarcoma arising in a solitary osteochondroma of the fibula. Arch Pathol Lab Med. 1999;123:832–4.
29. Florez B, Monckeberg J, Castillo G, Beguiristain J. Solitary osteochondroma long-term follow-up. J Pediatr Orthop B. 2008;17:91–4.
30. Hoshi M, Takami M, Hashimoto R, Okamoto T, Yanagida I, Matsumura A, et al. Spontaneous regression of osteochondromas. Skeletal Radiol. 2007;36:531–4.
31. Bernard SA, Murphey MD, Flemming DJ, Kransdorf MJ. Improved differentiation of benign osteochondromas from secondary chondrosarcomas with standardized measurement of cartilage cap at CT and MR imaging. Radiology. 2010;255:857–65.
32. Woertler K, Lindner N, Gosheger G, Brinkschmidt C, Heindel W. Osteochondroma: MR imaging of tumor-related complications. Eur Radiol. 2000;10:832–40.
33. Lee KC, Davies AM, Cassar-Pullicino VN. Imaging the complications of osteochondromas. Clin Radiol. 2002;57:18–28.
34. Brien EW, Mirra JM, Kerr R. Benign and malignant cartilage tumors of bone and joint: their anatomic and theoretical basis with an emphasis on radiology, pathology and clinical biology. I. The intramedullary cartilage tumors. Skeletal Radiol. 1997;26:325–53.
35. Marco RA, Gitelis S, Brebach GT, Healey JH. Cartilage tumors: evaluation and treatment. J Am Acad Orthop Surg. 2000;8:292–304.
36. Flemming DJ, Murphey MD. Enchondroma and chondrosarcoma. Semin Musculoskelet Radiol. 2000;4:59–71.
37. Ryzewicz M, Manaster BJ, Naar E, Lindeque B. Low-grade cartilage tumors: diagnosis and treatment. Orthopedics. 2007;30:35–46. quiz 47–38.
38. Douis H, Davies AM, James SL, Kindblom LG, Grimer RJ, Johnson KJ. Can MR imaging challenge the commonly accepted theory of the pathogenesis of solitary enchondroma of long bone? Skeletal Radiol. 2012; doi:10.1007/s00256-012-1387-4.
39. Amary MF, Bacsi K, Maggiani F, Damato S, Halai D, Berisha F, et al. IDH1 and IDH2 mutations are frequent events in central chondrosarcoma and central and periosteal chondromas but not in other mesenchymal tumours. J Pathol. 2011;224:334–43.
40. Kransdorf MJ, Peterson JJ, Bancroft LW. MR imaging of the knee: incidental osseous lesions. Magn Reson Imaging Clin N Am. 2007;15:13–24.
41. Levy JC, Temple HT, Mollabashy A, Sanders J, Kransdorf M. The causes of pain in benign solitary enchondromas of the proximal humerus. Clin Orthop Relat Res. 2005:181–186.
42. Walden MJ, Murphey MD, Vidal JA. Incidental enchondromas of the knee. AJR Am J Roentgenol. 2008;190:1611–5.
43. Lopez-Martin N, De Miguel I, Calvo E. Rotator cuff impingement due to enchondroma of the acromion. Acta Orthop Belg. 2005;71:732–5.
44. Shenoy R, Pillai A, Reid R. Tumours of the hand presenting as pathological fractures. Acta Orthop Belg. 2007;73:192–5.
45. Potter BK, Freedman BA, Lehman Jr RA, Shawen SB, Kuklo TR, Murphey MD. Solitary epiphyseal enchondromas. J Bone Joint Surg Am. 2005;87:1551–60.
46. Jones KB, Buckwalter JA, Frassica FJ, McCarthy EF. Intracortical chondroma: a report of two cases. Skeletal Radiol. 2006;35:298–301.
47. deSantos LA, Spjut HJ. Periosteal chondroma: a radiographic spectrum. Skeletal Radiol. 1981;6:15–20.
48. Robinson P, White LM, Sundaram M, Kandel R, Wunder J, McDonald DJ, et al. Periosteal chondroid tumors: radiologic evaluation with pathologic correlation. AJR Am J Roentgenol. 2001;177:1183–8.
49. Woertler K, Blasius S, Brinkschmidt C, Hillmann A, Link TM, Heindel W. Periosteal chondroma: MR characteristics. J Comput Assist Tomogr. 2001;25:425–30.
50. Matsushima K, Matsuura K, Kayo M, Gushimiyagi M. Periosteal chondroma of the rib possibly associated with hemothorax: a case report. J Pediatr Surg. 2006;41:E31–3.
51. Sinha S, Singhania GK, Campbell AC. Periosteal chondroma of the distal radius. J Hand Surg Br. 1999;24:747–9.
52. Hagiwara Y, Hatori M, Abe A, Tanaka K, Kokubun S. Periosteal chondroma of the fifth toe—a case report. Ups J Med Sci. 2004;109:65–70.
53. Peidro L, Suso S, Alcantara E, Ramon R. Periosteal chondroma of the clavicle. Skeletal Radiol. 1996;25:406–8.
54. Ricca Jr RL, Kuklo TR, Shawen SB, Vick DJ, Schaefer RA. Periosteal chondroma of the cuboid presenting in a 7-year-old-boy. Foot Ankle Int. 2000;21:145–9.
55. Ishida T, Iijima T, Goto T, Kawano H, Machinami R. Concurrent enchondroma and periosteal chondroma of the humerus mimicking chondrosarcoma. Skeletal Radiol. 1998;27:337–40.
56. Yamamoto Y, Washimi O, Yamada H, Washimi Y, Itoh M, Kuroda M. Concurrent periosteal chondroma and enchondroma of the fibula mimicking chondrosarcoma. Skeletal Radiol. 2006;35:302–5.
57. Emecheta IE, Bernhards J, Berger A. Carpal enchondroma. J Hand Surg Br. 1997;22:817–9.
58. An YY, Kim JY, Ahn MI, Kang YK, Choi HJ. Enchondroma protuberans of the hand. AJR Am J Roentgenol. 2008;190:40–4.
59. Dobert N, Menzel C, Ludwig R, Berner U, Diehl M, Hamscho N, et al. Enchondroma: a benign osseous lesion with high F-18 FDG uptake. Clin Nucl Med. 2002;27:695–7.
60. Geirnaerdt MJ, Hermans J, Bloem JL, Kroon HM, Pope TL, Taminiau AH, et al. Usefulness of radiography in differentiating enchondroma from central grade 1 chondrosarcoma. AJR Am J Roentgenol. 1997;169:1097–104.
61. Murphey MD, Flemming DJ, Boyea SR, Bojescul JA, Sweet DE, Temple HT. Enchondroma versus chondrosarcoma in the appendicular skeleton: differentiating features. Radiographics. 1998;18:1213–37. quiz 1244–1215.
62. Weiner SD. Enchondroma and chondrosarcoma of bone: clinical, radiologic, and histologic differentiation. Instr Course Lect. 2004;53:645–9.
63. Geirnaerdt MJ, Hogendoorn PC, Bloem JL, Taminiau AH, van der Woude HJ. Cartilaginous tumors: fast contrast-enhanced MR imaging. Radiology. 2000;214:539–46.
64. Skeletal Lesions Interobserver Correlation among Expert Diagnosticians (SLICED) Study Group. Reliability of histopathologic and radiologic grading of cartilaginous neoplasms in long bones. J Bone Joint Surg Am 2007;89:2113–23.
65. Eefting D, Schrage YM, Geirnaerdt MJ, Le Cessie S, Taminiau AH, Bovee JV, et al. Assessment of interobserver variability and histologic parameters to improve reliability in classification and grading of central cartilaginous tumors. Am J Surg Pathol. 2009;33:50–7.
66. Bui KL, Ilaslan H, Bauer TW, Lietman SA, Joyce MJ, Sundaram M. Cortical scalloping and cortical penetration by small eccentric chondroid lesions in the long tubular bones: not a sign of malignancy? Skeletal Radiol. 2009;38:791–6.
67. Kendell SD, Collins MS, Adkins MC, Sundaram M, Unni KK. Radiographic differentiation of enchondroma from low-grade chondrosarcoma in the fibula. Skeletal Radiol. 2004;33:458–66.
68. Gajewski DA, Burnette JB, Murphey MD, Temple HT. Differentiating clinical and radiographic features of enchondroma and secondary chondrosarcoma in the foot. Foot Ankle Int. 2006;27:240–4.

69. Davila JA, Amrami KK, Sundaram M, Adkins MC, Unni KK. Chondroblastoma of the hands and feet. Skeletal Radiol. 2004;33:582–7.
70. Ramappa AJ, Lee FY, Tang P, Carlson JR, Gebhardt MC, Mankin HJ. Chondroblastoma of bone. J Bone Joint Surg Am. 2000;82-A:1140–5.
71. Suneja R, Grimer RJ, Belthur M, Jeys L, Carter SR, Tillman RM, et al. Chondroblastoma of bone: long-term results and functional outcome after intralesional curettage. J Bone Joint Surg Br. 2005;87:974–8.
72. Lin PP, Thenappan A, Deavers MT, Lewis VO, Yasko AW. Treatment and prognosis of chondroblastoma. Clin Orthop Relat Res. 2005;438:103–9.
73. Fink BR, Temple HT, Chiricosta FM, Mizel MS, Murphey MD. Chondroblastoma of the foot. Foot Ankle Int. 1997;18:236–42.
74. Schuppers HA, van der Eijken JW. Chondroblastoma during the growing age. J Pediatr Orthop B. 1998;7:293–7.
75. Viswanathan S, Jambhekar NA, Merchant NH, Puri A, Agarwal M. Chondroblastoma of bone—not a " benign disease": clinicopathologic observations on sixty cases. Indian J Pathol Microbiol. 2004;47:198–201.
76. Rybak LD, Rosenthal DI, Wittig JC. Chondroblastoma: radiofrequency ablation—alternative to surgical resection in selected cases. Radiology. 2009;251:599–604.
77. Maheshwari AV, Jelinek JS, Song AJ, Nelson KJ, Murphey MD, Henshaw RM. Metaphyseal and diaphyseal chondroblastomas. Skeletal Radiol. 2011;40:1563–73.
78. Hameed MR, Blacksin M, Das K, Patterson F, Benevenia J, Aisner S. Cortical chondroblastoma: report of a case and literature review of this lesion reported in unusual locations. Skeletal Radiol. 2006;35:295–7.
79. Ozkoc G, Gonlusen G, Ozalay M, Kayaselcuk F, Pourbagher A, Tandogan RN. Giant chondroblastoma of the scapula with pulmonary metastases. Skeletal Radiol. 2006;35:42–8.
80. Gebert C, Hardes J, Streitburger A, Vieth V, Burger H, Winkelmann W, et al. Chondroblastoma of the acromion mimicking fibrous dysplasia. Acta Orthop Belg. 2004;70:616–8.
81. Mayo-Smith W, Rosenberg AE, Khurana JS, Kattapuram SV, Romero LH. Chondroblastoma of the rib. A case report and review of the literature. Clin Orthop Relat Res. 1990;230-4.
82. Matsuno T, Hasegawa I, Masuda T. Chondroblastoma arising in the triradiate cartilage. Report of two cases with review of the literature. Skeletal Radiol. 1987;16:216–22.
83. Akai M, Tateishi A, Machinami R, Iwano K, Asao T. Chondroblastoma of the sacrum. A case report. Acta Orthop Scand. 1986;57:378–81.
84. Singh J, James SL, Kroon HM, Woertler K, Anderson SE, Jundt G, et al. Tumour and tumour-like lesions of the patella—a multicentre experience. Eur Radiol. 2009;19:701–12.
85. Harish K, Janaki MG, Alva NK. “Primary” aggressive chondroblastoma of the humerus: a case report. BMC Musculoskelet Disord. 2004;5:9.
86. Zafatayeff-Hasbani S, Ducou Le Pointe H, Josset P, Damsin JP, Montagne JP. Intra-articular recurrence of benign chondroblastoma with articular involvement at initial presentation—a case report. Eur J Pediatr Surg. 2006;16:291–3.
87. Jambhekar NA, Desai PB, Chitale DA, Patil P, Arya S. Benign metastasizing chondroblastoma: a case report. Cancer. 1998;82:675–8.
88. Bloem JL, Mulder JD. Chondroblastoma: a clinical and radiological study of 104 cases. Skeletal Radiol. 1985;14:1–9.
89. Brower AC, Moser RP, Kransdorf MJ. The frequency and diagnostic significance of periostitis in chondroblastoma. AJR Am J Roentgenol. 1990;154:309–14.
90. Humphry A, Gilday DL, Brown RG. Bone scintigraphy in chondroblastoma. Radiology. 1980;137:497–9.
91. Hamada K, Ueda T, Tomita Y, Higuchi I, Inoue A, Tamai N, et al. False positive 18F-FDG PET in an ischial chondroblastoma; an analysis of glucose transporter 1 and hexokinase II expression. Skeletal Radiol. 2006;35:306–10.
92. Quint LE, Gross BH, Glazer GM, Braunstein EM, White SJ. CT evaluation of chondroblastoma. J Comput Assist Tomogr. 1984;8:907–10.
93. Weatherall PT, Maale GE, Mendelsohn DB, Sherry CS, Erdman WE, Pascoe HR. Chondroblastoma: classic and confusing appearance at MR imaging. Radiology. 1994;190:467–74.
94. Oxtoby JW, Davies AM. MRI characteristics of chondroblastoma. Clin Radiol. 1996;51:22–6.
95. Yamamura S, Sato K, Sugiura H, Iwata H. Inflammatory reaction in chondroblastoma. Skeletal Radiol. 1996;25:371–6.
96. Jee WH, Park YK, McCauley TR, Choi KH, Ryu KN, Suh JS, et al. Chondroblastoma: MR characteristics with pathologic correlation. J Comput Assist Tomogr. 1999;23:721–6.
97. Kaim AH, Hugli R, Bonel HM, Jundt G. Chondroblastoma and clear cell chondrosarcoma: radiological and MRI characteristics with histopathological correlation. Skeletal Radiol. 2002;31:88–95.
98. Lersundi A, Mankin HJ, Mourikis A, Hornicek FJ. Chondromyxoid fibroma: a rarely encountered and puzzling tumor. Clin Orthop Relat Res. 2005;439:171–5.
99. Schajowicz F, Gallardo H. Chondromyxoid fibroma (fibromyxoid chondroma) of bone. A clinico-pathological study of thirty-two cases. J Bone Joint Surg Br. 1971;53:198–216.
100. Beggs IG, Stoker DJ. Chondromyxoid fibroma of bone. Clin Radiol. 1982;33:671–9.
101. Wilson AJ, Kyriakos M, Ackerman LV. Chondromyxoid fibroma: radiographic appearance in 38 cases and in a review of the literature. Radiology. 1991;179:513–8.
102. Yamaguchi T, Dorfman HD. Radiographic and histologic patterns of calcification in chondromyxoid fibroma. Skeletal Radiol. 1998;27:559–64.
103. Sharma H, Jane MJ, Reid R. Chondromyxoid fibroma of the foot and ankle: 40 years' Scottish bone tumour registry experience. Int Orthop. 2006;30:205–9.
104. Fujiwara S, Nakamura I, Goto T, Motoi T, Yokokura S, Nakamura K. Intracortical chondromyxoid fibroma of humerus. Skeletal Radiol. 2003;32:156–60.
105. Takenaga RK, Frassica FJ, McCarthy EF. Subperiosteal chondromyxoid fibroma: a report of two cases. Iowa Orthop J. 2007;27:104–7.
106. Baker AC, Rezeanu L, O'Laughlin S, Unni K, Klein MJ, Siegal GP. Juxtacortical chondromyxoid fibroma of bone: a unique variant: a case study of 20 patients. Am J Surg Pathol. 2007;31:1662–8.
107. Song DE, Khang SK, Cho KJ, Kim DK. Chondromyxoid fibroma of the sternum. Ann Thorac Surg. 2003;75:1948–50.
108. Mizuno K, Sasaki T, Prado G, Saito Y, Kakizaki H, Matsumoto K, et al. Chondromyxoid fibroma of the scapula associated with aneurysmal bone cyst. Radiat Med. 1999;17:383–7.
109. Macdonald D, Fornasier V, Holtby R. Chondromyxoid fibroma of the acromium with soft tissue extension. Skeletal Radiol. 2000;29:168–70.
110. Nakazora S, Kusuzaki K, Matsumine A, Seto M, Fukutome K, Uchida A. Case report: chondromyxoid fibroma arising at the clavicular diaphysis. Anticancer Res. 2003;23:3517–22.
111. Brat HG, Renton P, Sandison A, Cannon S. Chondromyxoid fibroma of the sacrum. Eur Radiol. 1999;9:1800–3.